JOURNAL OF AIRCRAFT
Vol. 31, No. 5, Sept.–Oct. 1994

Analysis of an Oscillating Joukowski Airfoil with Surface Suction and Moving Vortices

Chyn-Shan Chiu*
China Junior College of Technology, Taipei, Taiwan. Republic of China

An attempt is made to enhance the beneficial effects of the trapped vortex by increasing its lingering period on the upper surface of a Joukowski airfoil in oscillating motions. Studies are made on the stability of a trapped free vortex when perturbed away from its equilibrium position with a finite displacement, and on the lingering period of the trapped free vortex in the upper vicinity of the airfoil. The computational results show that a proper combination of oscillation and suction might be an efficient method for trapping a free vortex to generate high lift on an airfoil. It is found that the trailing-edge suction position is more effective in capturing a free vortex for a longer lingering time and the lift increment directly dependent on the strength of the trapped vortex. This result may provide an explanation of the high lift generated by a dragonfly whose back wings are found to flap in a flow containing vortices shed from the front wings.

Nomenclature

A	= cross-sectional area
a	= radius
b	= half-chord length
g	= radius of gyration
k_j, k_r	= vortex strength
M	= moment about the midchord
m	= source strength
n	= total number of vortices
p, r	= pth and rth discrete vortex, respectively
$R(\tau + \Delta\tau)$	= corrector
$R_p(\tau)$	= predictor
T	= period
U	= freestream speed, reference speed
u, v	= complex speed component
W	= complex potential
X, Y	= force component in X and Y direction, respectively
$\dot{x}$, $\dot{y}$	= velocity component in X and Y direction, respectively
Z	= physical domain
$\bar{Z}$	= conjugate of Z
α	= angle of attack
$\dot{\alpha}$, ω	= angular velocity
$\ddot{\alpha}$	= angular acceleration
Γ	= circulation
$\Delta\alpha$	= angle increment
$\Delta\tau$	= time increment
ζ, ζ'	= computational domain
θ_s	= angular suction coordinate
μ, δ, β	= mapping parameters as shown in Fig. 2
ρ	= fluid density
τ	= dimensionless time

Introduction

FOR two-dimensional inviscid potential flow over a wing with a free vortex standing above the wing, Huang and Chow[1] showed that the lift on the wing can be increased significantly by the trapped vortex. The stationary vortex captured above the upper surface of the airfoil is typically unstable, and only some locations above the trailing edge are stable according to a linearized stability analysis. The effects of increasing angle of attack as well as increasing camber are to diminish the vortex-trapping ability of the airfoil and to reduce the magnitude of the maximum lift that can be produced by the trapped vortex. By increasing thickness, the trailing-edge vortex is stabilized, although it reduces the attainable maximum lift of the airfoil.

It is interesting to note to what extent the vortex lift already existed, and to develop new methods for more effective utilization of vortex-augmented lift. In 1973, it was claimed that a lift coefficient of 3.15 had been achieved by a glider by generating and maintaining spanwise vortices on the upper surface of the wing.[2] Then, Rossow[3] demonstrated analytically and experimentally that a free vortex could be trapped by a vertical flap near the leading edge while a suction was applied along the vortex axis. Saffman and Sheffield[4,5] treated this problem in a relatively simple way. They used the geometry of the airfoil to capture the vortex. Also, Ham[6] developed a general theory for the unsteady aerodynamic loading on an airfoil during dynamic stall. Sears[7] pointed out that the viscous and inviscid models of the unsteady airfoil are identical as long as the thin boundary layer in the viscous model remains attached to the airfoil surface all the way to the trailing edge. It was first postulated by Rossow[8] that the optimum way to trap a vortex is to design the airfoil section and wing so that the flow along the vortex core is minimized. Meanwhile, he showed that a vertical fence both in front of and behind the separation bubble generated by the trapped vortex was an effective way to reduce the mass flow removal and its associated drag to a negligible amount.

Studies of flows about an unsteady airfoil have been motivated mostly by efforts to avoid or reduce such undesirable effects as flutter, vibrations, buffeting, gust response, and dynamic stall. But it is well known that the vortices produced by separation at sharp leading edges can increase the lift on an airfoil for delta wings and similar low-aspect-ratio airfoils. Fairly extensive literature on vortex-induced high lift for a slender wing can be found in Refs. 5 and 9. The concept of using vortices for control of wake turbulence and for insect flight has also been investigated.[10,11] From these earlier works, an attempt has been made to enhance the beneficial effects of the trapped vortex by releasing intermittently from the upper surface of an airfoil.[12] Now the author is continuing efforts to increase the lingering period on the upper surface of the airfoil.

Received May 5, 1993; revision received Oct. 25, 1993; accepted for publication Nov. 20, 1993.

*Associate Professor and Director, Department of Mechanical Engineering, 245, Sec. 3 Yenchiuyuan Rd.

General Theory and Computational Procedure

When an airfoil is put suddenly at a certain angle of attack in a uniform flow, a vortex sheet is shed from the trailing edge. This continuous wake vortex sheet can be approximated by a row of discrete line vortices. Their displacements are then calculated and the vortices redistributed on the new distorted sheet. Although vortices observed in the laboratory are most likely formed from the rolling up of vortex sheets resulting from boundary-layer separation at the sharp tip of the spoiler or rotor as sketched in Fig. 1, they are treated as discrete potential vortices based on inviscid incompressible flow analysis.[12]

As shown in Fig. 2, the transformation[1]

$$z = \{[\zeta + (b^2/\zeta)]/2\} \tag{1}$$

$$\zeta = \zeta' + \delta e^{i\mu} \tag{2}$$

map a circle of radius a centered at the origin of the ζ' plane into a Joukowski airfoil in the z plane, whose chord is slightly longer than $2b$. The shape of the airfoil is controlled by changing the parameters δ and μ. That is, the generally cambered airfoil becomes a symmetrical airfoil when $\mu = \pi$; it becomes a circular arc when $\mu = (\pi/2)$; and it transforms into a flat plate for $\delta = 0$. The point $\zeta = b$ maps into the sharp trailing edge of the airfoil in all cases. The radius a and the angle β shown in Fig. 2 can be expressed in terms of the above two parameters as

$$a^2 = b^2 + \delta^2 - 2b\delta \cos \mu \tag{3}$$

$$\tan \beta = [\delta \sin \mu/(b - \delta \cos \mu)] \tag{4}$$

Under the same transformations, the uniform flow of constant speed $(U/2)$ making an angle α_0 with the horizontal axis maps into the uniform flow of constant speed U without changing its orientation. On the other hand, a line vortex k_j and a sink $-2m$ will keep the same strength through the transformations. In order to satisfy the boundary condition that the flow be tangent to the circle and to fulfill Kelvin's theorem of constant total circulation, the transformations must be done as shown in Fig. 2. For the vortex k_j, an image vortex of strength $-k_j$, and another vortex of strength k_j are added at $(a^2/\bar{\zeta}'_j)$ and the origin of the circle, respectively. Likewise, for the sink $-2m$, m is added at the origin, and another equal strength m is added at infinity.

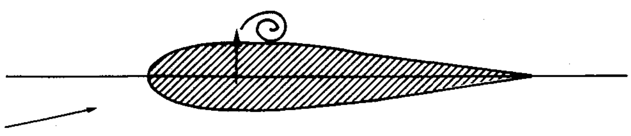

Fig. 1 Vortex generated behind an oscillating spoiler or rotating rotor.

Suppose the initial steady-state circulation about the airfoil is Γ, its value is determined by the airfoil angle of attack α_0 at the onset of pitching motion and the strength and location of the surface suction.[13] After vortices have been generated by a perturbing mechanism, the total circulation in the entire flow must be kept at its initial value based on the inviscid theory. Even though a set of three vortices is added in the circle plane for each of the discrete vortices in the airfoil plane, the total circulation of all vortices situated at the origin of the circle in the circle plane must be Γ at all times, no matter how many vortices are produced in the flow. Consequently, it is sufficient to represent a vortex, either generated by a spoiler or shed in the wake, by a vortex pair in the circle plane. Thus, at any instant in time, the sum of the time-dependent bounded circulation around the airfoil Γ_τ, and the total circulation of vortices in the fluid $\Sigma_{j=1}^{n} k_j$, is therefore a constant, i.e.,

$$\Gamma = \Gamma_\tau + \sum_{j=1}^{n} k_j \tag{5}$$

According to Milne-Thomson,[14] if a transformed unit circular cylinder is moving with a speed U making an angle α with the ξ axis, and at the same time is rotating with counterclockwise angular velocity ω about a center of rotation with the transformed circle, the complex potential without circulation is the sum of the negative powers of ζ in the expression

$$-Uze^{-i\alpha} + U\bar{z}e^{i\alpha} + i\omega z\bar{z} \tag{6}$$

Here, $z = f(\zeta)$, $f(\zeta)$ is the transformation function between the physical plane and the unit circle plane. Let the approximate half-chord b be the reference length, the freestream speed U be the reference speed, (b/U) be the reference time, and bU be the reference circulation and the reference poten-

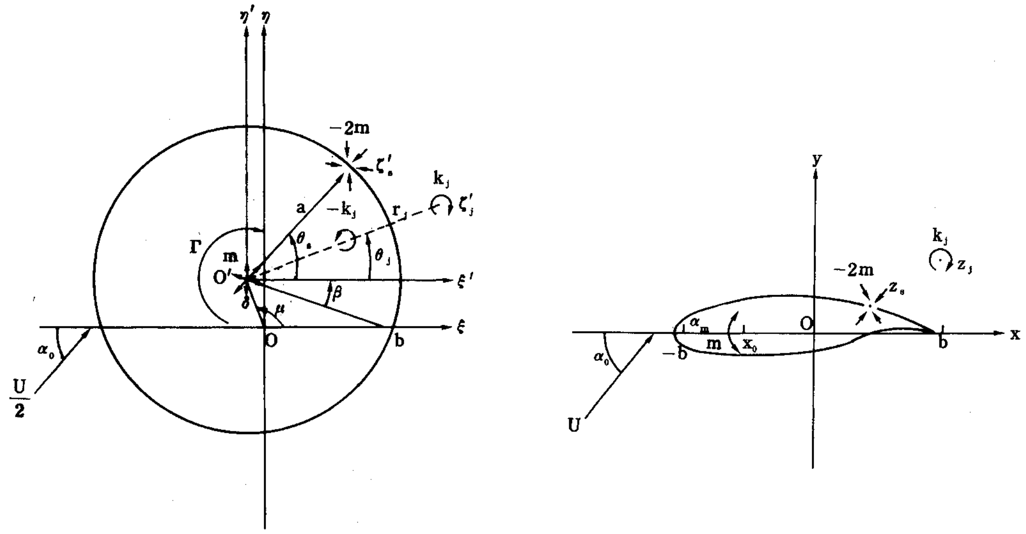

Fig. 2 Transformation of the flow about a circle into that about a Joukowski airfoil.

tial per unit length. The dimensionless complex potential at any point ζ' is

$$W(\zeta') = \frac{1}{2}\left(\zeta' e^{-i\alpha} + \frac{a^2}{\zeta'} e^{i\alpha}\right) + \frac{i\dot{\alpha}[(a^2/\zeta') + \delta e^{-i\mu}]}{4(\zeta' + \delta e^{i\mu})} - \frac{i\dot{\alpha}x_0}{2}\left(\frac{a^2}{\zeta'} + \frac{1}{\zeta' + \delta e^{i\mu}}\right) + \frac{i\Gamma}{2\pi}\log\zeta' + \sum_{j=1}^{n}\frac{ik_j}{2\pi}\left[\log(\zeta' - \zeta_j') - \log\left(\zeta' - \frac{a^2}{\bar{\zeta}_j'}\right)\right] - \frac{m}{2\pi}[2\log(\zeta' - \zeta_s') - \log\zeta'] \tag{7}$$

The complex speed of the flow in the physical plane, at any point other than the trailing edge of the airfoil or the center of a discrete vortex, is

$$\dot{x} - i\dot{y} = \frac{dW}{dz} = \frac{dW}{d\zeta'}\bigg/\frac{d\zeta}{d\zeta'}\bigg/\frac{dz}{d\zeta} \tag{8}$$

in which

$$\frac{dW}{d\zeta'} = \frac{1}{2}\left(e^{-i\alpha} - \frac{a^2 e^{i\alpha}}{\zeta'^2}\right) - \frac{i\dot{\alpha}}{4(\zeta' + \delta e^{i\mu})^2}\left(\frac{2a^2}{\zeta'} + \frac{a^2\delta e^{i\mu}}{\zeta'^2} + \delta e^{i\mu}\right) + \frac{i\dot{\alpha}x_0}{2}\left[\frac{a^2}{\zeta'^2} + \frac{1}{(\zeta' + \delta e^{i\mu})^2}\right] + \frac{i\Gamma}{2\pi\zeta'} + \sum_{j=1}^{n}\frac{ik_j}{2\pi}\left[\frac{1}{\zeta' - \zeta_j'} - \frac{1}{\zeta' - (a^2/\bar{\zeta}_j')}\right] - \frac{m}{2\pi}\left(\frac{2}{\zeta' - \zeta_s'} - \frac{1}{\zeta'}\right) \tag{9}$$

$$\frac{d\zeta}{d\zeta'} = 1, \qquad \frac{dz}{d\zeta} = \frac{1}{2}\left(1 - \frac{1}{\zeta^2}\right) \tag{10}$$

$$\alpha = \alpha_0 + \alpha_0 \sin 2\pi\tau \tag{11}$$

For general unsteady airfoil problems it is possible to obtain the unique numerical solutions by imposing either the condition of finite velocities about the trailing edge or the condition of zero loading about the trailing edge.[15] In the present theory, the Joukowski airfoil has a cusp at the trailing edge where the upper and lower surfaces are tangent. The Kutta condition for this type of edge is that the velocity there is finite. In Eq. (9) it demands that $(dW/d\zeta') = 0$ at $\zeta = 1$. Based on this boundary condition, the strength of the rth nascent vortex that has just been shed in the wake at position ζ_r' can be found as

$$K_r = \frac{2\pi a\sin(\alpha + \beta) + \pi a\dot{\alpha}[a + \delta\cos(\mu + \beta) - 2x_0\cos\beta] - \Gamma - \sum_{j\neq r}^{n}\dfrac{k_j(a^2 - \zeta_j'\bar{\zeta}_j')}{(ae^{-i\beta} - \zeta_j')(ae^{i\beta} - \bar{\zeta}_j')}}{\dfrac{a^2 - \zeta_r'\bar{\zeta}_r'}{(ae^{-i\beta} - \zeta_r')(ae^{i\beta} - \bar{\zeta}_r')}} \tag{12}$$

The complex velocity at the trailing edge must be evaluated alternatively as the following, due to the fact that Eq. (8) is indeterminate there

$$(\dot{x} - i\dot{y})_{TE} = \frac{\left(\dfrac{d^2W}{d\zeta'^2}\right)\zeta' = ae^{-i\beta}}{\left(\dfrac{d^2z}{d\zeta^2}\right)\zeta = 1} \tag{13}$$

In Eq. (13) the denominator has a numerical value of unity, and the numerator is obtained from Eq. (7). Once in the wake, the rth nascent vortex is convected at the local fluid velocity without changing its strength.

On the other hand, the complex velocity at the center of the pth discrete vortex at z_p in the airfoil plane can be found as

$$(u - iv)z_p = \left[\frac{dW}{dz} - \frac{ik_p}{2\pi}\frac{1}{(z - z_p)}\right]z_p = \frac{\zeta_p^2}{(\zeta_p^2 - 1)}\left[\left(e^{-i\alpha} - \frac{a^2e^{i\alpha}}{\zeta_p'^2}\right) - \frac{i\dot{\alpha}}{2\zeta_p^2}\left(\frac{2a^2}{\zeta_p'} + \frac{a^2\delta e^{i\mu}}{\zeta_p'^2} + \delta e^{i\mu}\right) + i\dot{\alpha}x_0\left(\frac{a^2}{\zeta_p'^2} + \frac{1}{\zeta_p^2}\right) + \frac{i\Gamma}{\pi\zeta_p'} + \sum_{j\neq p}^{n}\frac{ik_j}{\pi}\frac{1}{\zeta' - \zeta_j'} - \sum_{j=1}^{n}\frac{ik_j}{\pi}\frac{1}{\zeta' - (a^2/\bar{\zeta}_j')} - \frac{m}{\pi}\left(\frac{2}{\zeta' - \zeta_s'} - \frac{1}{\zeta'}\right)\right] - \frac{ik_p}{\pi}\frac{\zeta_p}{(\zeta_p^2 - 1)^2} \tag{14}$$

Since the flow is analyzed with the reference to a coordinate system instantaneously fixed in the airfoil, the Blasius theorem and the Bernoulli equation must be written for a translating and rotating frame of reference.[14] With the moment positive in the sense of increasing angle of attack, the generalized Blasius theorem for an unsteady flow is rewritten as

$$X - iY = \frac{i\rho}{2}\int\left(\frac{dW}{dz}\right)^2 dz + \rho\dot{\alpha}\int(\bar{z} - x_0)\,d\bar{W} + i\rho\frac{\partial}{\partial t}\int\bar{W}\,d\bar{z} + \rho A x_0(\dot{\alpha}^2 - i\ddot{\alpha}) \tag{15}$$

$$M = \text{REAL}\left[\frac{\rho}{2}\int\left(\frac{dW}{dz}\right)^2 z\,dz + \rho\frac{\partial}{\partial t}\int Wz\,d\bar{z} - 2Ag^2\ddot{\alpha}\right] \tag{16}$$

Substituting W from Eq. (7) and integrating then nondimensionalized by $\rho U^2 b$ and $2\rho U^2 b^2$ for the forces and the moment, respectively. The final expressions for the forces and the moment are

$$C_X + iC_Y = e^{i\alpha}(m + i\Gamma) - \frac{\dot{\alpha}(\Gamma + im)}{2}(\delta e^{i\mu} - 2x_0) + i\pi\dot{\alpha}e^{-i\alpha} + \frac{\pi(\dot{\alpha}^2 + i\ddot{\alpha})}{4}[\delta e^{-i\mu} - 2x_0(a^2 + 1)] - \sum_{j=1}^{n}\frac{ik_j}{2}\left[\frac{(u + iv)z_j}{\left(\dfrac{dz}{d\zeta}\right)\zeta_j} + \frac{a^2}{\bar{\zeta}_j'^2}\frac{(u - iv)_{zj}}{\left(\dfrac{dz}{d\zeta}\right)\bar{\zeta}_j}\right] - \sum_{j=1}^{n}\frac{\dot{\alpha}k_j}{2}\left[\zeta_j' - \frac{a^2}{\bar{\zeta}_j'} - 2(z - x_0)\right] + Ax_0(\dot{\alpha}^2 + i\ddot{\alpha}) \tag{17}$$

$$C_M = \text{REAL}\left\{\frac{\pi\dot{\alpha}e^{-i\alpha}}{8}\left[\delta e^{-i\mu} - 2x_0(a^2 + 1) + a^2\delta e^{i\mu}\left(\frac{e^{i2\mu}}{\delta^2} - 1\right)\right] + \frac{e^{-i\alpha}}{4}\left[\frac{i\pi e^{-i\alpha}}{2} - \delta e^{i\mu}(\Gamma + im)\right] - \sum_{j=1}^{n}\frac{k_je^{-i\alpha}}{4}\left(\zeta_j' - \frac{a^2}{\bar{\zeta}_j'}\right) + \sum_{j=1}^{n}\frac{k_jz_j}{2}(u - iv)z_j - Ag^2\ddot{\alpha}\right\} \tag{18}$$

The force coefficients C_X and C_Y are decomposed further into the drag and lift coefficients as

$$C_D + iC_L = (C_X + iC_Y)e^{-i\alpha} \tag{19}$$

They act, respectively, in the directions parallel and perpendicular to the instantaneous velocity vector of the airfoil.

The pressure on the airfoil must be calculated by using the unsteady Bernoulli equation. Referred to the moving axes defined previously, the pressure coefficient is

$$C_p = 1 - 2\frac{\partial \phi}{\partial t} - q_r^2 + q^2 \tag{20}$$

in which

$$q_r^2 = \left| \frac{\mathrm{d}W}{\mathrm{d}z} - i\dot{\alpha}(\bar{z} - x_0) \right|^2 \tag{21}$$

$$q^2 = \dot{\alpha}^2 |z - x_0|^2 \tag{22}$$

$$\frac{\partial \phi}{\partial t} = \mathrm{REAL} \left\{ \frac{-i\dot{\alpha}}{2}\left(\zeta' e^{-i\alpha} - \frac{a^2 e^{i\alpha}}{\zeta'}\right) + \frac{i\ddot{\alpha}}{4\zeta}\left(\frac{a^2}{\zeta'} + \delta e^{-i\mu}\right) - \frac{i\ddot{\alpha}x_0}{2}\left(\frac{a^2}{\zeta'} + \frac{1}{\zeta}\right) - \sum_{j=1}^{n} \frac{ik_j}{2\pi}\left[\frac{1}{\zeta' - \zeta_j'} \frac{(u + iv)z_j}{\left(\frac{\mathrm{d}z}{\mathrm{d}\zeta}\right)\zeta_j} + \frac{1}{\zeta' - \frac{a^2}{\bar{\zeta}_j'}} \frac{a^2}{\bar{\zeta}_j'^2} \frac{(u - iv)z_j}{\left(\frac{\overline{\mathrm{d}z}}{\mathrm{d}\zeta}\right)\bar{\zeta}_j}\right]\right\} \tag{23}$$

Finally, we consider the coordinate transformation after the z coordinate system rotated through an angle $\Delta\alpha$ about the point x_0 after a small time increment Δ_τ. The new position of the origin relative to the original z coordinate system is given by

$$z_0 = x_0(1 - \cos \Delta\alpha) + ix_0 \sin \Delta\alpha \tag{24}$$

Then, the location of a point z_j^N following an angular displacement $\Delta\alpha$ of the reference axes about z_0 in terms of the former location of the point z_j^{N-1} is

$$z_j^N = (z^N - z_0)e^{-i\Delta\alpha} \tag{25}$$

The computational procedure for obtaining the present solution is based on the above general theory. For numerical computations, we choose $\mu = \pi$ and $\delta = 0.15$ to obtain a 17% thick symmetrical Joukowski airfoil of chord $c = 2.035$ in the dimensionless physical plane, and a circle of radius $a = 1.15$ with $\beta = 0$ in the dimensionless circle plane. The strength of each of the vortices generated by a perturbing device is normally determined by the size of the device, frequency of oscillation, Reynolds number, and other factors. However, since no previously published results corresponding to the present case can be used, the strength is assigned an arbitrary value of 0.5 for all of the examined cases. For example, at time $\tau = 0$, the first vortex of circulation $k_1 = 0.5$ is released at a fixed position z_1 above the airfoil. Instantaneously a wake vortex is shed in order to make the flow smooth at the trailing edge.

For a sink of given suction strength that is placed at a fixed position on the upper surface of the airfoil at an angle of attack, a vortex can be trapped at various locations above the airfoil, depending upon the strength of the vortex.[13] In the present problem the suction strength is arbitrarily set at $m = 0.1$, and is placed at three different positions on the upper surface of the airfoil by choosing θ_s to be 1.0, $(\pi/2)$, and 3.0 radians, respectively. For simplicity, these positions will be called, respectively, the trailing-edge, midchord, and leading-edge positions of the surface suction. In addition, the center of oscillation is set by letting $x_0 = 0$ in the present case.

The solution for the vortical flow about the oscillating airfoil with surface suction undergoing an arbitrary time-dependent, simple-harmonic motion that started at $\tau = 0$ is calculated at successive intervals of time. An increment $\Delta\tau$ is chosen as 2.5% of the oscillating period so that one cycle of oscillation is completed in 40 time steps. The new position of a vortex is calculated by a two-step predictor-corrector procedure as

$$\boldsymbol{R}_p(\tau) = \boldsymbol{R}(\tau) + \Delta\tau \boldsymbol{V}[\boldsymbol{R}(\tau)] \tag{26}$$

$$\boldsymbol{R}(\tau + \Delta\tau) = \boldsymbol{R}(\tau) + (\Delta\tau/2)\{\boldsymbol{V}[\boldsymbol{R}(\tau)] + \boldsymbol{V}[\boldsymbol{R}_p(\tau)]\} \tag{27}$$

Where $\boldsymbol{R}(\tau)$ is the previous position, $\boldsymbol{R}_p(\tau)$ is the predictor, $\boldsymbol{R}(\tau + \Delta\tau)$ is the new position, and $\boldsymbol{V}$ is the velocity vector.

At the end of that time increment, a new vortex is shed in the wake. Instead of assuming its location as in the case of the first shed vortex, it is assumed at a distance $u_{\mathrm{TE}}\Delta\tau$ downstream from the trailing edge on the x axis, where u_{TE} is the x component of Eq. (13). With this position known, the strength of this shed vortex can be computed according to Eq. (12).

Numerical computations described previously are then repeated until a desired time level is reached. The number of wake vortices is increased by 1 at the end of each iteration. The tip of the wake vortex rolls into a spiral, which becomes tighter and tigher as time progresses. When distances among vortices become too close, inaccurate results are expected that appear in the form of scattered vortices in the wake. In order to eliminate the chaotic motion of the discrete wake vortices, Moore's method[16] is used to combine the first two into one concentrated tip vortex, situated at their centroid position, when the total number of shed wake vortices exceeds a certain value in the computation. Based on many tries, a maximum number of 20 vortices in the wake is the proper choice for saving computer time, and yet the results so obtained are still reliable. It is found that increasing the total number of wake vortices in the computation will cause the free vortex to shift a short distance downward during its passing over the upper surface of the airfoil. In computing the solution after each time increment $\Delta\tau$, the locations of all vortices relative to the airfoil after having rotated through an angle $\Delta\alpha$ are computed using Eq. (24).

Results and Discussion

As shown in Ref. 13, the position of a trapped vortex around a stationary airfoil is determined by the freestream speed, strength of the vortex, the shape of the airfoil, as well as an arbitrary suction strength and its location. A free vortex can also be trapped instantaneously at various locations around an oscillating airfoil. In order to examine the stability of the trapped vortex above an oscillating airfoil, it intentionally disturbed a finite displacement from its instantaneous equilibrium position. It found that usually the vortex moves toward the trailing edge, and in the meantime turns into a higher location than the latest one in their corresponding trajectory when (τ/π) become bigger. But sometimes the vortex moves in the upstream direction first, and then turns back and moves away from the upper surface of the airfoil.

Based on the criterion for stability, the amplitude of the vortex motion does not grow with time; it may either return to the equilibrium point or circle around it. In the present example, the vortex still tends to circle around the stationary point, but with an increasing radius after a displaced finite amplitude. It is concluded, after examining many cases, that all of the instantaneous equilibrium positions of the trapped vortex are unstable to finite disturbances, but in some configurations it may stay longer on the upper surface of the airfoil.

Table 1 Lingering period of a vortex when it is released at z_1 above an oscillating airfoil with surface suction

Parameter	θ_s	δ	μ	m	x_0	τ	α	z_1, k_1, starting position and circulation	τ/π, lingering period
Leading-edge trajectory	1.0	0.15	π	0.10	0.0	π	0 deg + 5 deg sin $2\pi\tau$	$-0.698 + i0.219$; 0.907	20.570
	$\pi/2$	0.13	π	0.10	0.0	π	0 deg + 5 deg sin $2\pi\tau$	$-0.088 + i0.693$; 9.283	4.550
	3.0	0.18	π	0.10	-0.5	π	0 deg + 5 deg sin $2\pi\tau$	$-0.397 + i0.520$; 5.041	2.665
Trailing-edge trajectory	1.0	0.15	π	0.15	-0.5	π	0 deg + 5 deg sin $2\pi\tau$	$0.202 + i0.429$; 5,278	>220.275
	$\pi/2$	0.15	π	0.10	0.0	π	0 deg + 5 deg sin $2\pi\tau$	$0.545 + i0.372$; 5.550	5.770
	3.0	0.13	π	0.10	0.0	π	0 deg + 2.5 deg sin $2\pi\tau$	$0.627 + i0.306$; 4.631	4.115

Note: z_1 and k_1 from stationary position without oscillation.

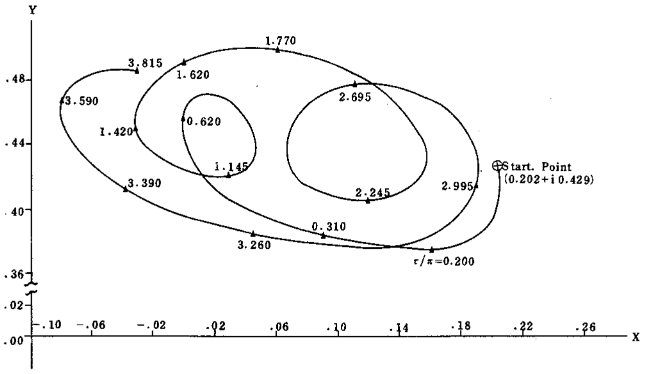

Fig. 3 Trajectories of a vortex of circulation 5.278 after it is released at its stationary point ⊕ above an oscillating airfoil, $\alpha = 0$ deg + 5 deg sin $2\pi\tau$, $T = \pi$, $x_0 = -0.5$, $m = 0.15$ and $\theta_s = 1.0$, as seen in the nonrotating coordinate system.

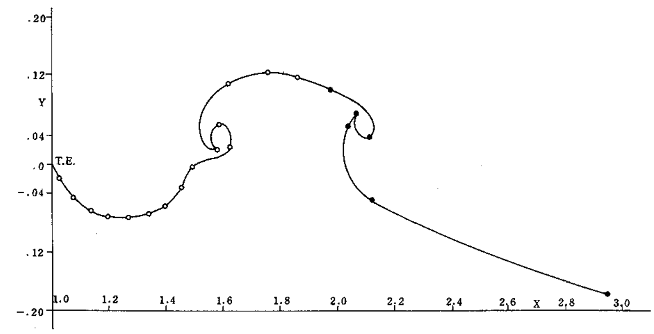

Fig. 4 Wake pattern at $\tau = 1.995\pi$ when the vortex moves along the trajectory shown in Fig. 3; (○) for vortex of clockwise circulation and (●) for vortex of counterclockwise circulation.

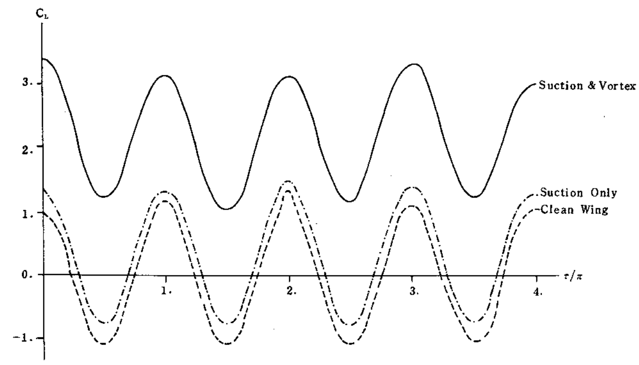

Fig. 5 Comparison of lift coefficient variation with time for cases of suction and vortex, suction only, and clean wing when the vortex moves along the trajectory shown in Fig. 3.

The computational procedure described previously is now used to find the right combinations of oscillation, suction, and airfoil geometry that can make a free vortex linger above the airfoil for a longer period of time in order to generate a higher lift. Therefore, all possible parameters in the governing equation, such as airfoil thickness, suction strength and location, pitching amplitude and center, vortex starting position, etc., will be considered in the maximization process. To start the computation it is assumed that $\alpha = 0$ deg + 5 deg sin $2\pi\tau$, $T = \pi$, $\delta = 0.15$, $\mu = \pi$, $x_0 = 0$, $\theta_s = (\pi/2)$, and $m = 0.1$. The free vortex starts from its instantaneous equilibrium position that is determined by θ_s, and the size of time step $\Delta\tau$ in the computation is automatically varied by the requirement that $u_v\Delta\tau$ be less than 0.008. In the subsequent numerical computations the above-mentioned parameters are changed one by one until a long lingering period is obtained.

Among all the cases that have been tested, some representative results are tabulated in Table 1. When the vortex of strength $k = 5.278$ at the equilibrium position $z = 0.202 + i0.429$ with initial circulation $\Gamma = 2.314$, $x_0 = -0.5$, $m = 0.15$, and with the other parameters kept the same as the starting values, the trajectory in the first four pitching cycles is plotted in Fig. 3. Numerical computation shows that for this particular case the vortex still lingers in the vicinity of the upper surface of the airfoil after 220.275 pitching cycles. Since the CPU time for this case is 2451.35 s on a Cyber 170-720 computer, no attempt has been made to extend the computation.

Figure 3 shows that the vortex lingers in a random manner instead of following a regular locus, due to the complicated contributions from all the governing parameters. The aerodynamic performance of the airfoil and the wake pattern of the present case are also examined. Figure 4 reveals the rolling-up of the wake vortices; the pattern closely resembles those obtained numerically in Refs. 15, 17, and 18, and those observed in real fluid shown in Ref. 19. It shows that the first 15 shed vortices have clockwise circulations, and the following six vortices have counterclockwise circulations when $\tau = 1.995\pi$. Note that the wake element immediately following the trailing edge is virtually parallel to both the upper and the lower airfoil surface, and so the present solution completely satisfies the Kutta condition.

Variations of lift, drag, and moment coefficients with time are plotted in Figs. 5–7 for cases of a clean airfoil, an airfoil with surface suction, and that with the captured vortex. Figure 5 indicates that, when the strong vortex of strength $k = 5.278$ is captured above the airfoil, the lift is positive and higher than those in the other two cases over the early four cycles of oscillation. Even though the instantaneous angle of attack is between 5 and -5 deg, the lift is always higher than 1.0 over the whole pitching cycle. This result suggests an efficient method to enhance the lift of an airfoil by trapping a free vortex using oscillation and surface suction. When the vortex is captured above the oscillating airfoil, the drag oscillates with a large amplitude at the frequency of the airfoil motion. Variations of drag with time are plotted in Fig. 6. Note that the magnitude of drag is two-order smaller than that of lift

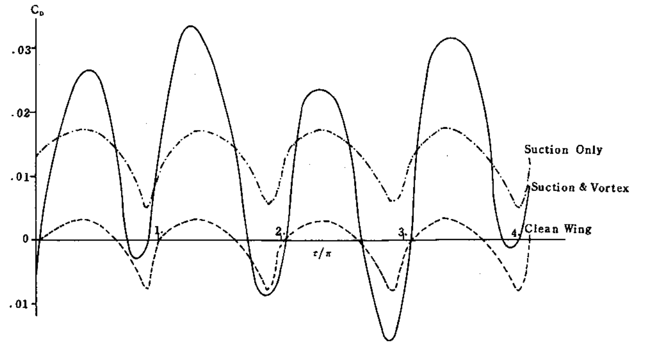

Fig. 6 Comparison of drag coefficient variation with time for cases of suction and vortex, suction only, and clean wing when the vortex moves along the trajectory shown in Fig. 3.

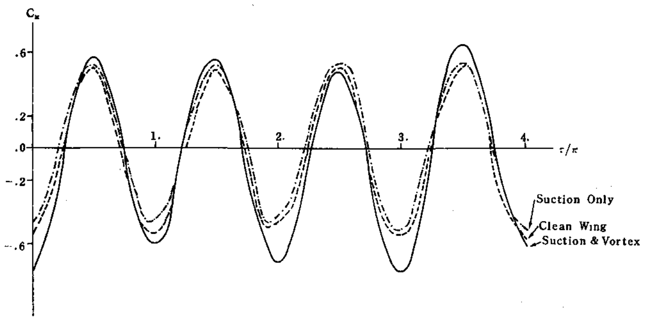

Fig. 7 Comparison of moment coefficient variation with time for cases of suction and vortex, suction only, and clean wing when the vortex moves along the trajectory shown in Fig. 3.

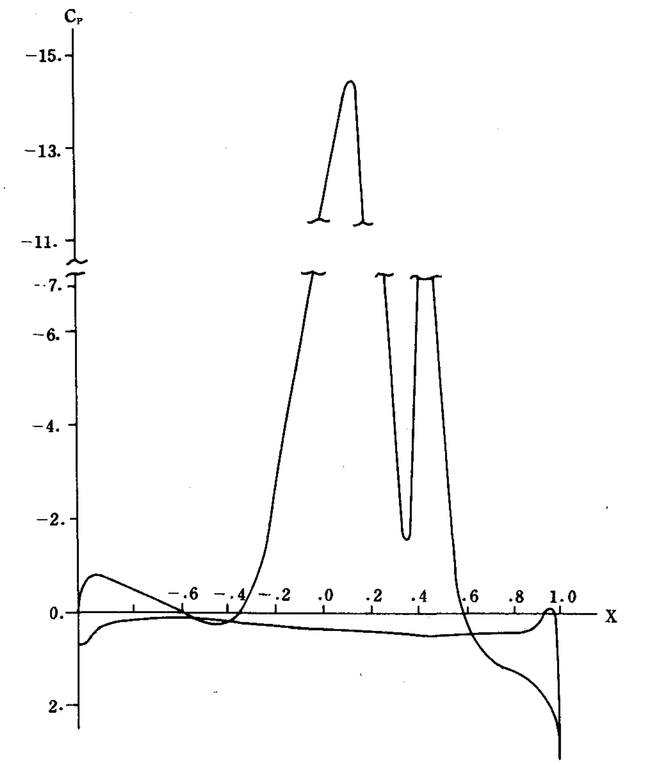

Fig. 8 Pressure distribution around the airfoil at $\tau = 1.995\pi$ when the vortex moves along the trajectory shown in Fig. 3.

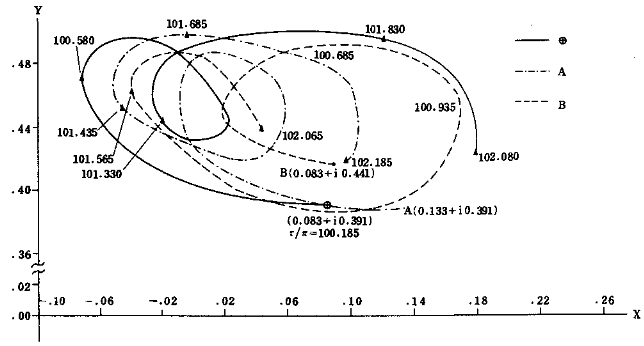

Fig. 9 Trajectories of a lingering vortex when it is displaced from its instantaneous position ⊕ to points A and B after the airfoil has oscillated 100.185 cycles with all parameters shown in Fig. 3.

in all three cases. Figure 7 shows that the moment coefficients in all three cases oscillate at the same frequency as that of the airfoil with a very small difference in amplitude.

The pressure distribution around the airfoil in the present problem is plotted in Fig. 8 at $\tau = 1.995\pi$ when the airfoil has a maximum lift. The pressure on the lower surface is generally higher than that on the upper surface, except in a small region near the trailing edge. A finite low pressure directly below the vortex and an infinite low pressure at the sink are also found on the upper surface of the airfoil. It is seen that the low-pressure region below the vortex is wider than that at the sink.

Finally, to investigate the stability of this lingering vortex, the vortex is perturbed from its instantaneous position, after the airfoil has oscillated 100.185 cycles, to point A through a horizontal displacement $\Delta x = 0.05$, or to point B through a vertical displacement $\Delta y = 0.025$. Figure 9 reveals that in either case the disturbed vortex goes into an alternative trajectory lingering above the airfoil, showing that the vortex is neutrally stable to those small disturbances. This behavior of the vortex suggests that the application of both oscillation and surface suction on an airfoil could be an effective technique to capture a free vortex stably for generating high unsteady lift on the airfoil. Although the present method is different from Ref. 8, the work on the use of a vortex trapped above a wing in order to produce high lift at low angles of attack is the same. In an actual application, the author believes that some withdrawal of fluid at the center of the vortex is needed to help render the equilibrium or zero-velocity condition at the center of the vortex, as stated by Rossow.

Conclusions

To examine the effect of surface suction, an arbitrarily chosen suction of strength $m = 0.1$ is applied on an airfoil whose shape is defined by $\delta = 0.15$ and $\mu = \pi$. Sink locations are varied by letting $\theta_s = 1.0$, $(\pi/2)$, and 3.0, all in radians, which correspond respectively to 72.4%, 44.4%, and chord distances measured horizontally from the leading edge. Influences of suction on the lingering period of the trapped vortex are summarized in Table 1. As shown, the trailing-edge suction position is more effective in capturing a free vortex for a longer lingering time. Nevertheless, the best case found in the present example is obtained by increasing the suction strength m from 0.10 to 0.15, and shifting the pitching center to quarterchord.

To the dynamic problem of vortical flows about an oscillating airfoil, the lingering period of the trapped free vortex is an encouraging feature for the present study. The problem is solved by the method of circle-airfoil conformal mapping technique under the assumption that the fluid is inviscid and incompressible. Vortex trajectory, wake pattern, surface suction effects, pressure distributions, and force and moment coefficients have been presented for an oscillating symmetrical Joukowski airfoil.

The main objective of this study was to develop a new method for more effective utilization of the beneficial effects of the trapped vortex on the upper surface of a Joukowski airfoil. Although there are many parameters in the governing equations, a proper combination of them has been found that enables a free vortex to stay above an oscillating airfoil for a long period of time. Interestingly, in the presence of the trapped moving vortex, the lift is always positive and the drag may even become negative, although the angle of attack oscillates between −5–5 deg. It is thus found that the lingering of the trapped free vortex can greatly improve the lift of the airfoil. This result may provide an explanation of the high lift generated by a dragonfly, whose back wings are found to flap in a flow containing vortices shed from the front wings, as evidenced by the flow visualization photographs in Refs. 20 and 21.

References

[1]Huang, M.-K., and Chow, C.-Y., "Trapping of a Free Vortex by Joukowski Airfoil," *AIAA Journal*, Vol. 20, No. 3, 1982, pp. 292–298.

[2]Cox, J., "The Revolutionary Kasper Wing," *Soaring*, Vol. 37, Dec. 1973, pp. 20–30.

[3]Rossow, V. J., "Lift Enhancement by an Externally Trapped Vortex," *Journal of Aircraft*, Vol. 15, No. 9, 1978, pp. 618–625.

[4]Saffman, P. G., and Sheffield, J. S., "Flow over a Wing with an Attached Free Vortex," *Studies in Applied Mathematics*, Vol. 57, 1977, pp. 107–117.

[5]Sheffield, J. S., "Topics in Vortex Motion," Ph.D. Dissertation, California Inst. of Technology, Pasadena, CA, 1978.

[6]Ham, N. D., "Aerodynamic Loading on a Two-Dimensional Airfoil During Dynamic Stall," *AIAA Journal*, Vol. 6, No. 10, 1986, pp. 1927–1934.

[7]Sears, W. R., "Unsteady Motion of Airfoils with Boundary-Layer Separation," *AIAA Journal*, Vol. 14, No. 2, 1976, pp. 216–220.

[8]Rossow, V. J., "Two-Fence Concept for Efficient Trapping of Vortices on Airfoil," *Journal of Aircraft*, Vol. 29, No. 5, 1992, pp. 847–855.

[9]Polhamus, E. C., "Predictions of Vortex-Lift Characteristics by a Leading-Edge Suction Analogy," *Journal of Aircraft*, Vol. 8, 1971, pp. 193–199.

[10]Landahl, M. T., and Widnall, S. E., "Vortex Control," *Aircraft Wake Turbulence and Its Detection*, edited by Olsen, Goldberg, and Rogers, Plenum Press, New York, 1971, pp. 137–156.

[11]Maxworthy, T., "The Fluid Dynamics of Insect Flight," *Annual Review of Fluid Mechanics*, Vol. 13, 1981, pp. 329–350.

[12]Chow, C.-Y., and Chiu, C.-S., "Unsteady Loading on Aircraft Due to Vortices Released Intermittently from Its Surface," *Journal of Aircraft*, Vol. 23, No. 10, 1986, pp. 750–755.

[13]Chow, C.-Y., Chen, C.-L., and Huang, M.-K., "Trapping of Free Vortex by Airfoils with Surface Suction," AIAA Paper 85-0446, Jan. 1985.

[14]Milne-Thomson, L. M., *Theoretical Hydrodynamics*, 5th ed., Macmillan, New York, 1968, pp. 240–267.

[15]Basu, B. C., and Hancock, G. J., "The Unsteady Motion of a Two-Dimensional Aerofoil in Incompressible Inviscid Flow," *Journal of Fluid Mechanics*, Vol. 87, Pt. 1, 1978, pp. 159–178.

[16]Moore, D. W., "A Numerical Study of the Roll-Up of a Finite Vortex Sheet," *Journal of Fluid Mechanics*, Vol. 63, 1974, pp. 225–235.

[17]McCrosky, W. J., "Unsteady Airfoils," *Annual Review of Fluid Mechanics*, Vol. 14, 1982, pp. 285–311.

[18]Giesing, J. P., "Nonlinear Two-Dimensional Unsteady Potential Flow with Lift," *Journal of Aircraft*, Vol. 5, March–April 1968, pp. 135–143.

[19]Van Dyke, M., *An Album of Fluid Motion*, Parabolic Press, Stanford, CA, 1982, pp. 56–57.

[20]Somps, C. J., "Lift Generation Mechanisms of the Dragonfly," AIAA Region V Student Conference in St. Louis, MO, April 1982.

[21]Savage, S. B., Newman, B. G., and Wang, T.-M., "The Role of Vortices and Unsteady Effects During the Hovering Flight of Dragonflies," *Journal of Experimental Biology*, Vol. 83, 1983, pp. 59–77.